

Principles of Visual Tokens for Efficient Video Understanding

Xinyue Hao¹ Gen Li¹ Shreyank N Gowda² Robert B Fisher¹ Jonathan Huang³
Anurag Arnab Laura Sevilla-Lara¹

¹University of Edinburgh ²University of Nottingham ³Scaled Foundations

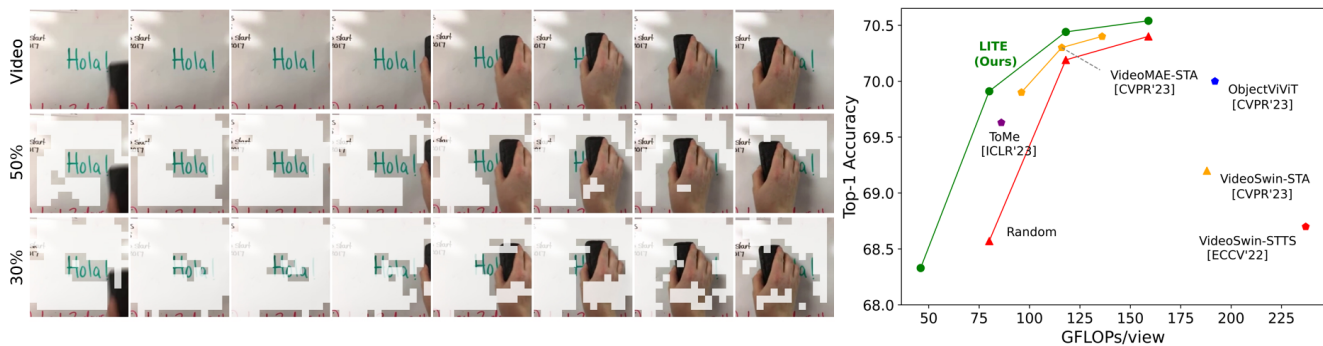


Figure 1. Left: Given an input video, the proposed LITE method is able to select a subset (non-white patches) of discriminative tokens for any given computational budget. Right: LITE is lightweight and efficient, outperforming state-of-the-art in the trade-off between computational cost (GFLOPs) and accuracy. The plot shows the results on Something-Something-V2.

Abstract

Video understanding has made huge strides in recent years, relying largely on the power of the transformer architecture. As this architecture is notoriously expensive and video is highly redundant, research into improving efficiency has become particularly relevant. This has led to many creative solutions, including token merging and token selection. While most methods succeed in reducing the cost of the model and maintaining accuracy, an interesting pattern arises: most methods do not outperform the random sampling baseline. In this paper we take a closer look at this phenomenon and make several observations. First, we develop an oracle for the value of tokens which exposes a clear Pareto distribution where most tokens have remarkably low value, and just a few carry most of the perceptual information. Second, we analyze why this oracle is extremely hard to learn, as it does not consistently coincide with visual cues. Third, we observe that easy videos need fewer tokens to maintain accuracy. We build on these and further insights to propose a lightweight video model we call LITE that can select a small number of tokens effectively, outperforming state-of-the-art and existing baselines across datasets (Kinetics400 and Something-Something-V2) in the challenging trade-off of computation (GFLOPs) vs accuracy.

1. Introduction

Video understanding has made remarkable progress in the last few years, getting close to solving many standard benchmarks and tasks. This progress has largely hinged on the use of the transformer architecture [36], which is both extremely powerful as well as extremely computationally expensive. Transformers originated in the language field, where few tokens are needed to represent a concept, for example an action, as tokens roughly correspond to single words. This is not the case in the visual adaptation of transformers [1], where the number of tokens to represent an action is orders of magnitude larger, leading to an exponentially larger computational cost. This cost has a wide range of negative consequences: it limits the deployability of models, as they require expensive equipment to run, it burdens video understanding research, making turnaround slower, it is financially expensive and it has a big environmental footprint [16]. In particular, although the inference cost is small compared to training, over the lifetime of a model, the overall cost of inference is larger than the cost of training, as it is done many more times [28]. At the same time, video is notoriously redundant both in space (where background regions might be a large part of the scene) and time (with many frames being similar, even if they are downsampled from the original video). These two

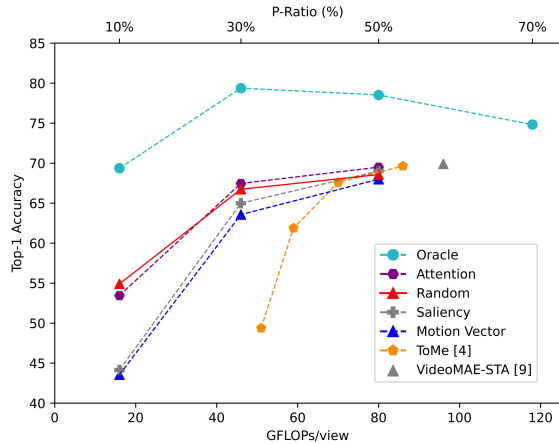


Figure 2. **Random sampling of tokens** is comparable to or outperforms most sophisticated models for token selection, as well as other sampling baselines. The “P-Ratio” represents the proportion of tokens selected relative to the total number of tokens per video.

factors together pose a great opportunity opening a research theme on token reduction. This theme has led to many creative ideas on how to reduce the amount of tokens. One of the noticeable strands is token-merging, where similar tokens are grouped together such that only a representative of the group needs to be stored in memory [4, 8, 9, 14]. Other ideas have revolved around selecting tokens based on motion, such as the Motionformer [27]. These models can reduce the computational cost in GFLOPs considerably, while keeping accuracy on-par with the full model.

Crucially, we observe that most of these models make a trade-off between accuracy and computation that is similar or inferior to the simplest baseline of sampling tokens randomly (see Fig. 2). In this paper we take a closer look at this puzzling effect, and discover some underlying principles of the nature of visual tokens that are useful for designing faster, more efficient video models.

Using a subset of “good” tokens can be better than using all tokens. First, we design an oracle that estimates the value of each token for a particular task, concretely we take *Action Classification* as our testbed. This oracle is created such that the value of each input token corresponds to its gradient [32]. We refer to it as an oracle because it uses the ground truth label of the class. Given this oracle, we can now sample a subset of the tokens according to their gradient value, keeping those with higher values. We observe that the accuracy of using a subset of tokens of a video according to the oracle is actually much larger than the baseline of using all tokens. In other words, “low-value” tokens not only do not help, but actually act as noise that hurt classification. Crucially, this gap is also shockingly large: it can be up to 9%. This demonstrates even further the surprising value of the oracle.

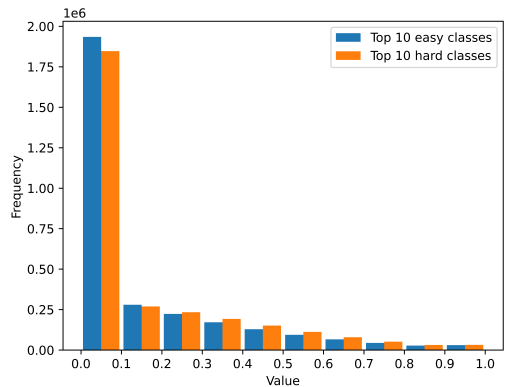


Figure 3. **Histogram of value of tokens** as predicted by the oracle, showing a very clear Pareto-like distribution. Easy classes have thinner tails than hard classes.

The value of tokens follows a Pareto distribution. We can plot a histogram of the value of tokens estimated by our oracle and observe that it closely follows a Pareto distribution, where the vast majority of tokens carry a very small amount of information, while a select few carry most of the information necessary for classification. This helps explain the puzzling power of the random-drop baseline: when sampling randomly, we are more likely to discard from valueless pile, therefore less likely to affect the overall performance of the model.

Searching for the right tokens is like looking for a needle in a haystack. What does the oracle’s performance look like? Does it attend to cues that humans use, such as foreground objects? Furthermore, can we train a simple model to reproduce the oracle? We conducted a series of experiments to understand the nature of the tokens selected by the oracle. We assess how they compared to those selected by other methods, including: selecting the foreground, selecting the regions with more attention, etc. Surprisingly, all these strategies perform much worse than selecting tokens at random. We then propose a “selector” network, which we call LITE for *Lightweight Token Elector*, which takes as input a token and approximates the value of the oracle. We observe that although the selector is extremely lightweight, it is enough to outperform previous work on token selection and merging, including the strong random-selection baseline. This selector is a simple multi-layer perceptron (MLP) which operates at the token level individually, and in our experiments no comparison methods give better performance.

Easy tasks do not need as much computation to maintain high accuracy. Easy classes tend to have token distributions with slightly thinner tails. This suggests that potentially there are fewer “essential” tokens for classification. We measure the impact of adapting the computational budget on a per-video basis, such that easier videos

(with high prediction confidence) use a smaller budget than harder videos (with low prediction confidence).

We make several **contributions**:

- We provide a comprehensive study of the nature of value of tokens in video, distilling our findings into 5 principles that can be leveraged for future research.
- We incorporate these principles into a novel method, LITE that is architecture-agnostic and task-agnostic, and can be used as plug-and-play for other settings.
- We advance the state-of-the-art in efficiency of video across standard datasets, maintaining accuracy while cutting over of GFLOPs.

2. Related Work

Video Transformers. Transformer-based architectures [36] have generally delivered outstanding improvements in various image-related tasks [10, 21, 35]. Beyond images, they have also spurred significant research in video understanding [1, 3, 6, 11, 17, 21, 23, 27, 40], yielding promising outcomes. However, the computational cost of Transformers increases quadratically with the number of tokens, which presents challenges for handling longer videos.

Efficient Video Recognition. Video Understanding has struggled with efficiency for years, spurring a big body of work on reducing input data [12, 13, 19, 41, 48], leveraging motion [27], or using a memory cache [42] to enable long-video analysis. Some recent work leverage advances in image models to adapt them to videos using parameter-efficient fine-tuning [24, 25, 38, 43].

Transformer Token Reduction. From all efficiency strategies, the most relevant to this work is reduction of tokens. Some methods drop tokens by predicting scores through end-to-end training [30, 37, 44]. For instance, DynamicViT [30] scores each token using a lightweight network and selects top tokens with Gumbel-softmax. A-ViT [44] computes halting scores from the token embedding’s first dimension to decide on pruning, while STTS [37] uses a differentiable Top- K operator to predict scores and select top areas for reduced computation.

Additionally, some methods extract essential information from all tokens to reduce their number [20, 26, 31]. Strategies like K -centered search [26] are used for this purpose. TokenLearner [31] employs MLPs to learn a fixed number of new tokens, thus reducing the computational load from processing numerous tokens. LookupVit [20] uses compressed tokens for high computational processing, and other tokens for cheaper layers.

Another mainstream approach is merging redundant or similar tokens [4, 8, 9, 14]. The seminal ToMe [4] method merges similar tokens using bipartite matching algorithms. Building on ToMe, STA [9] developed a video-specific to-

ken dropping method where the first frame uses ToMe, and each subsequent frame is compared with the remaining tokens from the previous frame, retaining similar ones. Additionally, the vid-TLDR [8] work incorporates a saliency mask based on ToMe, enhancing the contribution of tokens in salient areas in subsequent learning. Moreover, the recent STTM [14] method extracts object cues, compresses token information within the same object, and add aggregated position information to compensate for the loss of motion cues. A special case of token reduction is frame selection, which has led to a series of interesting work including SMART [15], Sevilla [45], Vila [39] and ATP [5].

Unlike previous data-centric approaches, LITE uses an oracle-driven, model-focused method to retain high-value tokens via direct gradient scoring, adapting compute based on video complexity to improve efficiency and accuracy over existing methods.

3. Principles of Visual Tokens in Video

In this section we take a closer look at the nature of visual tokens in video. The goal is to use the underlying principles to design an efficient model that can both reduce the computational complexity of models at test time as well as leverage the overwhelming redundancy of tokens in video. We introduce the experimental setup, including architectures, datasets, and implementation details used throughout the paper, followed by key principles and supporting experimental evidence.

Datasets. We use two standard action recognition datasets: Kinetics-400 [7], sourced from YouTube, is a large-scale human action video dataset with 400 classes. Each class has a minimum of 400 action clips. Something-Something V2 (SS-V2) [18] focuses on fine-grained understanding of human hand gestures. Comprising 220,847 labeled video clips, it captures 174 individuals performing predefined actions with everyday items. This dataset poses a greater challenge for temporal modeling [33].

Implementation Details. We use VideoMAE [34] as backbone as it is very widely used. Frames in each video are uniformly sampled and clips of size $16 \times 224 \times 224$ pixels are used as network inputs with a tube size of $2 \times 16 \times 16$. During inference, we use two temporal clips. For each temporal clip, we take three spatial crops (top-left, center, bottom-right) of size 224×224 pixels. The final prediction is obtained by averaging the scores from all views (temporal clips \times spatial crops). All experiments were carried out using 2 NVIDIA RTX 3090 24GB GPUs.

Principle 1: Random is better than most

First, we compare the current state-of-the-art to random token selection, using the SS-V2 dataset and the VideoMAE architecture. Figure 2 shows the trade-off between comput-

ing resources (GFLOPs) and accuracy. In this paper, we define P-Ratio as the percentage of tokens selected compared to the total number of tokens per video. Although recent work on token selection leverages many different cues to select discriminative tokens, surprisingly, the random baseline is comparable or superior to others like ToMe [4] or video-specific models [9] across all computational budgets.

Principle 2: Good tokens do not coincide with visual cues

It would seem that if selecting random tokens produces strong results, inserting some amount of bias should improve results. This would also show us what type of visual content correlates more with the important parts of the scene: is it foreground? Is it moving regions? We experiment with several possible baselines and show results shown in Fig. 2:

- **Attention:** We consider using the magnitude of the attention of each token at test time. Given that these are the cues that the model is actually “attending to” for classification, it seems like a strong signal to find good tokens. Still, it is remarkable that this is very much on-par with the random baseline.
- **Motion Vectors:** Motion tends to carry information about what are the discriminative regions of an action. Typically, regions that move tend to correspond to the foreground and therefore to the region where the action is taking place. In this baseline, we simply use the motion vectors (MVs) of the video, which come for free with the compressed video, and sample those that have the highest magnitude of motion. This baseline is also worse, especially for the lower computational budgets.
- **Saliency:** Finally we use a saliency detector CPFE [46] to compute the saliency at each frame. We then sample the tokens with highest saliency. Saliency turns out to not be better than random.

Principle 3: Low-value tokens can hurt recognition

Can we characterize good tokens and bad tokens? This would help us selecting them to reduce computational complexity. However, as just shown, reasonable inductive biases based on visual cues, such as motion, attention and saliency perform worse than the random selection of tokens. Here we try a different approach: what if we can use the gradient of each token in the video as a potential cue? This should show what parts of the video correlate more strongly with each specific class.

Designing an oracle to predict the value of tokens. To identify which tokens play a decisive role in the classification task and to assign a score to each token based on their importance, we design an oracle to predict the value of a given token, using Grad-CAM [32]. As mentioned before, we call this an oracle because it has access to privileged in-

formation – the true class label. However, this is indeed a tractable approximation of a “real oracle”, which would be to find the k -subset of tokens that minimizes the loss relative to the true label.

We first calculate the gradient of the score for the target class c , with respect to the feature map activations of the MLP in the last blocks:

$$\omega_d^c = \frac{1}{N} \sum_t \sum_h \sum_w \frac{\partial y^c}{\partial A_{thw}^d} \tag{1}$$

where y^c is the score before applying softmax for target class c , A_{thw}^d is the feature map activations at position $\{t, h, w\}$ with the feature d . After obtaining the gradient score, we perform average pooling across all tokens to derive an importance weight ω_d^c for each feature of the target class c . To approximate the ground truth as closely as possible and create a more accurate oracle, the target class selected here is the true label class.

After obtaining the importance weights for each feature, we calculate the importance score of each token for the target class using a linear combination. We incorporate a ReLU function when deriving the final token score to ensure that only tokens with a positive impact on the class are considered, making the activation maps clearer and concentrated:

$$S^c = ReLU \left(\sum_d \omega_d^c A^d \right) \tag{2}$$

where A^d is the feature map activations with the feature d , ω_d^c is the importance weight of feature d at target class c , and $S^c \in \mathbb{R}^{t \times h \times w}$ is the final token score for the target class c . Finally, we apply min-max normalization to scale all patch scores to a range between 0 and 1.

Testing the oracle. Is S^c a good oracle? We measure its accuracy by selecting the top- K tokens with highest value for several different computation budgets. We use SS-V2 as dataset and VideoMAE as the backbone. Results are shown in Fig. 2. We make two observations: first the oracle is much better than all other baselines, as well as the state-of-the-art. This is not necessarily surprising but it is reassuring that it is indeed a good way to measure the value of a token for recognition. We also observe that unlike other methods and baselines, the accuracy of the oracle does not strictly increase as we include more tokens. Instead, there is a sweet-spot, where high-value tokens have been chosen, but low-value, potentially noisy and confusing tokens have not been chosen. This is also an interesting insight, which gives us hope that this type of oracle can be instrumental for the design of efficient models. Figure 4 shows some sample masks of what the values of the oracle look like.

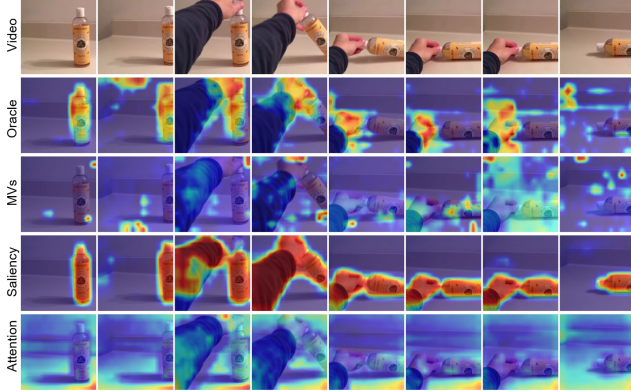


Figure 4. **Sample heatmaps for different visual cues.** From top to bottom: input video frames, oracle, magnitude of motion vectors, saliency, and attention.

Principle 4: The value of tokens follows a Pareto distribution

Figure 3 shows a histogram of the oracle’s token values for a large set of videos. This has a very Pareto-like distribution where most tokens carry little information and a few vital ones carry most of it. This helps explain the puzzling effectiveness of the random sampling: as long as some of the tail tokens are included in the random sample, the video can be classified correctly. Observing the shape of the accuracy curve for the random selector in Fig. 2, it is far from linear. We can see that there is a cliff when the percentage of sampled tokens is smaller than 30%. A plausible explanation is that at that point, the probability of sampling tail tokens becomes too small, and therefore it is significantly less likely that the video is classified correctly.

Principle 5: Easy videos require less compute

Figure 3 shows an additional insight: easier classes have thinner tails than harder classes. Even if the difference seems small, it is statistically significant, as the number of tokens analyzed is very large. This can potentially mean that there are greater numbers of important or essential tokens in the hard videos than in the easy ones, and therefore they might benefit from increasing the number of sampled tokens. To explore this hypothesis we plot, for each class, how the accuracy decreases with random sampling as a function of the original accuracy. This is seen in Fig. 5. We observe that for a given sampling ratio (50%), the accuracy of easier classes (*e.g.* those with higher baseline accuracy) is less affected than the accuracy of harder classes.

4. LITE

The findings of Sec. 3 point to two fundamental ideas that we can leverage to design a video model, LITE, that is lightweight, efficient and adaptive and outperforms the

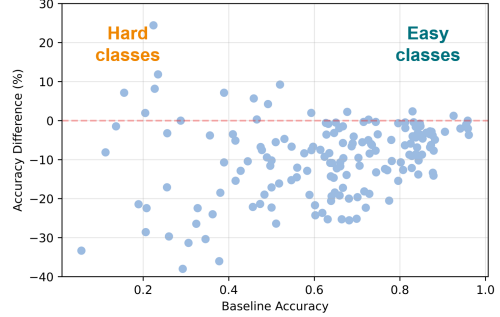


Figure 5. **Impact of dropping 70% of tokens in easy classes vs hard classes.** The X-axis is the accuracy when using all tokens. The Y-axis is the decay of the accuracy when dropping 70% of tokens, as a percentage. Easier classes suffer less when the computational budget is reduced.

strong random baseline as well as the previous state-of-the-art. These two fundamental ideas are 1) that the oracle is a reliable source of information about the value of a token and 2) that easy videos need less compute than hard videos. In this section we first review the standard Video Transformer model, which we use as backbone, and then describe how we integrate our two core ideas into LITE and show an overview of the model in Fig. 6. We then discuss other possible variants that we have experimented with.

4.1. Review of Video Transformer

Video Transformer takes as input a clip of video $\mathcal{V} \in \mathbb{R}^{T \times H \times W \times 3}$, which contains T RGB frames with the size of $H \times W$ sampled from the original video. Following the approach of ViT [10], Video Transformer flattens frames into N 3D patches with size $\{p_t, p_h, p_w\}$, where $N = \lfloor \frac{T}{p_t} \rfloor \times \lfloor \frac{H}{p_h} \rfloor \times \lfloor \frac{W}{p_w} \rfloor$. Thus, Video Transformer converts a video to a sequence of non-overlapping patches.

In this paper, patch n with temporal index t is represented as $\mathbf{v}_n^t \in \mathbb{R}^{3p_t \times p_h \times p_w}$, where $n = 1, \dots, N$ and $t = 1, \dots, \lfloor \frac{T}{p_t} \rfloor$. The patch embedding vector $\mathbf{z}_n^t \in \mathbb{R}^D$ is obtained by means of a learnable linear projection and a separate addition of spatio-temporal positional embedding.

$$\mathbf{z}_n^t = M\mathbf{v}_n^t + \mathbf{e}_n + \mathbf{e}^t \quad (3)$$

M is a learnable linear matrix and \mathbf{e}_n and \mathbf{e}^t are the separate spatial and temporal learnable positional embeddings. To model the appearance and motion in the video, each patch is processed with a stack of Transformer encoding blocks. In each block ℓ , the patch embedding is updated by multi-head attention (Attention), LayerNorm (LN), and MLP processes:

$$\hat{\mathbf{z}}_n^{t(\ell+1)} = \text{Attention} \left(\text{LN} \left(\mathbf{z}_n^{t(\ell)} \right) \right) + \mathbf{z}_n^{t(\ell)} \quad (4)$$

$$\mathbf{z}_n^{t(\ell+1)} = \text{MLP} \left(\text{LN} \left(\hat{\mathbf{z}}_n^{t(\ell+1)} \right) \right) + \hat{\mathbf{z}}_n^{t(\ell+1)} \quad (5)$$

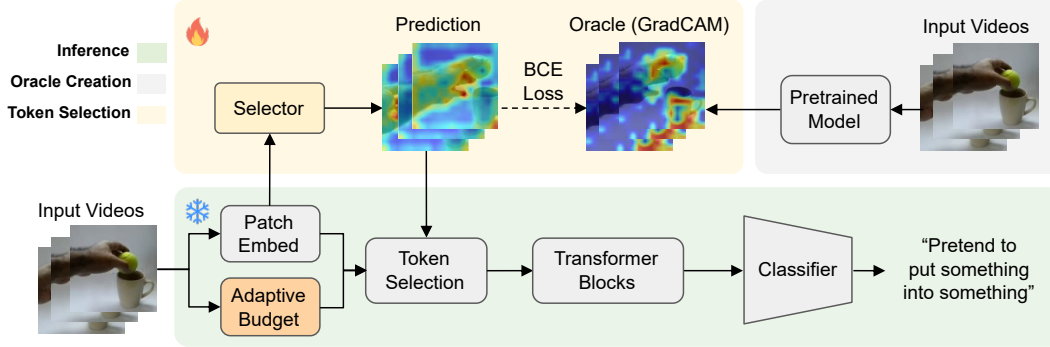


Figure 6. **Overview of LITE.** At training time, video gradients are used to build the oracle, which the selector learns to replicate. At test time, the predicted value of the selector is used to keep the top most useful tokens, reducing the overall burden of the input to the classifier.

where $\ell = 1, \dots, L - 1$ and L is the total number of blocks.

4.2. Learning to Select

Given the oracle concept, the goal is to design a lightweight selector that can predict the oracle’s value of each token. A necessary condition is that the model has to be lightweight, as it has to be significantly faster than using all tokens.

Assume a sequence of patch embeddings $\mathbf{p} \in \mathbb{R}^{N \times D}$ where N is length of the patch embedding sequence and D is the embedding dimension. To maintain simplicity and ensure the model remains lightweight, we used a three-layer fully connected (FC) network to predict token scores. Given that the scores in the oracle $s \in [0, 1]$, we also incorporated a sigmoid function for better estimation:

$$\mathbf{s}' = \text{Sigmoid}(\text{FC}(\mathbf{p}; \boldsymbol{\theta})) \in \mathbb{R}^{N \times 1}, \quad (6)$$

where $\mathbf{p} \in \mathbb{R}^{N \times D}$ is the patch embedding, $\boldsymbol{\theta}$ is the network weights, and $\mathbf{s}' \in \mathbb{R}^N$ is our estimated token score.

We train our selector in conjunction with the frozen patch embedding module from the backbone model, using binary cross-entropy loss between the selector’s and oracle’s token values. This is depicted in the yellow region of Fig. 6. During inference, we insert our selector between the patch embedding module and the first transformer block, utilizing all weights from the original backbone model except those of our selector. This is depicted in the green region of Fig. 6.

4.3. Adaptive Computational Budget

Principle 5 shows that not all videos or tasks need the same amount of computation, and easy ones need a smaller number of tokens. This is similar to the case of image recognition in human perception, where we perform certain tasks (such as detecting familiar objects) faster than harder tasks (such as classifying occluded objects) [29]. Here we explore the use of this principle as follows: we gauge the difficulty of each video in a very lightweight manner and use this information to compute an “adaptive budget”, which

will adapt the computational budget and save computation on “easy” videos. This process is depicted as the orange box in Fig. 6 and it is referred to in experiments as LITE++, as it focuses on further reducing computation at a minimal cost.

Concretely, we gauge difficulty using confidence of the prediction as a proxy for whether a particular video will be correctly classified. To estimate this confidence we use a lightweight model (MoviNet [19]), which is considerably less accurate but extremely fast. Given the estimated confidence \hat{c} , the budget will be selected as follows: for very low confidence ($\hat{c} < \tau_1$) it is accepted that this will be a very hard case, and will not invest extra tokens; for easy cases ($\hat{c} > \tau_2$) we use a small budget, as it is likely that they will be easy to get right; for everything in between we use the baseline budget. In our experiments we use the following hyperparameters: $\tau_1 = 0.1$ and $\tau_2 = 0.5$. For easy cases, we select top 30% of tokens when the P-Ratio is 0.5, 0.7, or 0.9, and top 20% of tokens when the P-Ratio is 0.3.

4.4. Model Variants

Looking at the simplicity of LITE, one could think that learning to predict the oracle is particularly easy and straightforward. After all, if an MLP can learn this, potentially a more sophisticated model should outperform it. This section describes the series of variants evaluated, which might give additional insights into the nature of the token-selection problem as well as showcase that it is far from trivial. Results for all these variants are shown in Sec. 5.

Cleaning the oracle training data. The examples in Fig. 4 suggest that the oracle is somewhat noisy. Could there be some artifacts that we could correct to improve the performance of the oracle? Several cleaning strategies for the oracle were explored:

- Edges. Since Grad-CAM often produces noisy high activation around image boundaries, we diminish the values on edges to reduce boundary artifacts.
- Isolated peaks. The raw value of the oracle often has iso-

lated peaks, which can misrepresent the true important areas. We remove small areas below a certain threshold.

- Sharpening the distribution. The original distribution of the oracle is often smooth. We transform oracle values to amplify the differences between high and low values, making the distribution more concentrated around 0 or 1.

Including global information. The LITE model assesses the value of a token based solely on the information of one token. This is a simplification of the way tokens are used, and overlooks qualities such as diversity of information, relationship, etc. We experimented with adding a global branch to LITE, where instead of simply using the value of a token in isolation, we use several 3D convolutions to acquire the nearby context information. Then, a self-attention operation is employed to capture long-range dependencies and model interactions between tokens, allowing the network to integrate global information effectively.

Adding complexity to the selector. A 3-layer MLP is a fairly simple model, and potentially we should be able to do better with a more sophisticated model. Adding layers or using other architectures can potentially lead to better results, even at the cost of an increased amount of computation. We experimented with several aspects. We used more layers (up to 5) to add capacity to the MLP. We also tried other architectures and replace the MLP with single or multiple transformer blocks. Surprisingly, none of these variants impact the result of the selector. Results are shown in the Supplemental Material.

5. Experiments

The experimental validation on LITE starts with comparing current state-of-the-art models on the mainstream datasets Kinetics-400 and SS-V2. We then describe a series of studies to understand its behavior, including modifying architectural components, backbones, the oracle, etc. Experiment settings are the same as from the previous Sec. 3. Overall we observe that LITE outperforms previous state-of-the-art and that despite its simplicity is robust and effective.

5.1. Comparison to State-of-the-art

Tables 1 (also shown in Fig. 1) and 2 show the results of LITE on SS-V2 and Kinetics-400 respectively. We make several observations.

First, LITE offers a better trade-off between computational cost and accuracy than prior methods. At fixed accuracy, LITE requires less compute, and at fixed compute, it achieves higher accuracy. For example, on the SS-V2 dataset, LITE uses only 40% of ObjectViViT [47]’s GFLOPs with similar accuracy. On Kinetics-400, LITE achieves comparable accuracy with 12% of the GFLOPs used by LookupViViT [20]. LITE also outperforms token-merging methods: compared to ToMe [4], it achieves sim-

| Category | Model | GFLOPs × views | Top-1 | Top-5 |
|-----------|----------------------------------|----------------|-------|-------|
| Backbones | TimeSformer-L [2] | 5549x1x3 | 62.40 | – |
| | Motionformer-L [27] | 1185x1x3 | 68.10 | – |
| | VideoSwin-B [22] | 321x1x3 | 69.60 | – |
| | VideoMAE [34] | 181x2x3 | 70.50 | 92.35 |
| Efficient | VideoSwin-STTS [37] | 237x1x3 | 68.70 | – |
| | VIT-B-STTM [14] | 345x1x1 | 56.50 | 83.90 |
| | ObjectViViT [47] | 192x2x3 | 70.00 | – |
| | ToMe ₁₂₈ [4] | 86x2x3 | 69.63 | – |
| | VideoMAE-STA ₄₈ [9] | 116x2x3 | 70.30 | – |
| | VideoSwin-STA ₃₂₀ [9] | 188x2x3 | 69.20 | – |
| Proposed | LookupViViT [20] | 376x4x3 | 59.60 | – |
| | VideoMAE-LITE ₉₀ | 159x2x3 | 70.54 | 92.38 |
| | VideoMAE-LITE ₇₀ | 118x2x3 | 70.44 | 92.30 |
| | VideoMAE-LITE ₅₀ | 80x2x3 | 69.91 | 91.99 |
| | VideoMAE-LITE ₃₀ | 46x2x3 | 68.33 | 90.87 |

Table 1. **Comparison to state-of-the-art on Something-Something-V2.** The subscript on LITE refers to the percentage of tokens retained, equivalent to (P-Ratio × 100). The “P-Ratio” represents the proportion of tokens selected relative to the total number of tokens per video.

| Category | Model | GFLOPs × views | Top-1 | Top-5 |
|-----------|--------------------------------|----------------|-------|-------|
| Backbones | TimeSformer-L [2] | 8353x1x3 | 80.70 | – |
| | Motionformer-L [27] | 1185x10x3 | 80.20 | – |
| | ViViT [1] | 3981x4x3 | 84.90 | – |
| | VideoMAE [34] | 181x5x3 | 81.25 | 94.99 |
| Efficient | VideoSwin-STTS [37] | 253x4x3 | 81.90 | – |
| | VIT-B-STTM [14] | 345x1x1 | 73.30 | 90.50 |
| | ToMe ₁₂₈ [4] | 86x5x3 | 79.95 | – |
| | VideoMAE-STA ₄₈ [9] | 116x5x3 | 81.10 | – |
| | LookupViViT [20] | 376x4x3 | 78.30 | – |
| Proposed | VideoMAE-LITE ₉₀ | 159x5x3 | 81.33 | 94.95 |
| | VideoMAE-LITE ₇₀ | 118x5x3 | 81.14 | 94.89 |
| | VideoMAE-LITE ₅₀ | 80x5x3 | 80.36 | 94.51 |
| | VideoMAE-LITE ₃₀ | 46x5x3 | 78.39 | 93.28 |

Table 2. **Comparison to state-of-the-art on Kinetics-400.** The subscript in LITE refers to the percentage of tokens retained.

ilar GFLOPs reduction with an accuracy gain of 0.3% on SS-V2 and 0.5% on Kinetics-400. Likewise, LITE slightly outperforms STA [9] at equivalent GFLOPs.

Second, LITE significantly reduces computation while maintaining accuracy, cutting GFLOPs by over 50% with only a 0.6% accuracy loss on SS-V2 — an excellent trade-off. Third, this pattern is consistent; on Kinetics-400, LITE saves over 50% GFLOPs with a 0.9% drop in accuracy.

5.2. Qualitative Results

Figure 7 illustrates the token selection of LITE. In conjunction with the results presented in Tables 1 and 2, it is evident that LITE effectively selects tokens beneficial to the model and discards those that could mislead classification. Additionally, observing the tokens selected by the oracle reveals that the combination of effective tokens is diverse rather than concentrated. This diversity partly explains why the simple MLP selector is effective in our method; its sim-

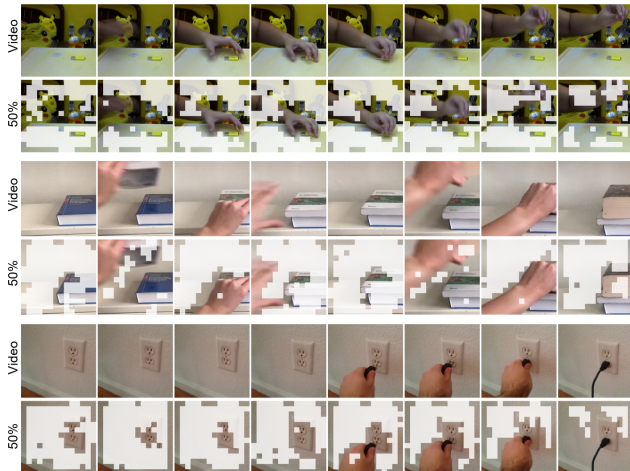


Figure 7. **Visualization of selected tokens** at 50% for different classes, including “Pretending to pick something up”, “Stacking number of something”, and “Plugging something into something”.

| Model | P-Ratio | GFLOPs | Top-1 | Top-5 |
|--------------------------|---------|--------|-------|-------|
| VideoMAE (baseline) | 1 | 181 | 70.50 | 92.35 |
| Oracle (true label) | 0.5 | 80 | 78.52 | 94.85 |
| Oracle (predicted label) | 0.5 | 80 | 70.00 | 91.25 |

Table 3. **Results using different labels to compute the gradient for the oracle.** Using the true label and sampling 50% of tokens produces much better results than even using all tokens.

| Model | GFLOPs \times views | Top-1 |
|-------------------------------|-------------------------|-----------------------|
| VideoMAE-LITE ₉₀ | 159x2x3 | 70.54 |
| VideoMAE-LITE++ ₉₀ | 105x2x3 _{↓34%} | 69.94 _{↓0.6} |
| VideoMAE-LITE ₇₀ | 118x2x3 | 70.44 |
| VideoMAE-LITE++ ₇₀ | 84x2x3 _{↓29%} | 69.86 _{↓0.6} |
| VideoMAE-LITE ₅₀ | 80x2x3 | 69.91 |
| VideoMAE-LITE++ ₅₀ | 65x2x3 _{↓19%} | 69.44 _{↓0.5} |
| VideoMAE-LITE ₃₀ | 46x2x3 | 68.33 |
| VideoMAE-LITE++ ₃₀ | 40x2x3 _{↓13%} | 67.74 _{↓0.6} |

Table 4. **Result comparison between LITE and LITE++.** In blue the reduced percentage of GFLOPs and accuracy.

plicity helps prevent the oracle from overfitting while preserving the ability to select a diverse range of tokens.

5.3. Analysis of LITE

Oracle creation. Gradient scores in the oracle can be calculated in two different ways: either using the true label or using the highest predicted class. Table 3 displays the performance of these two variants keeping 50% of tokens. We observe that using the true label provides a very large improvement of 8.5%.

Adaptive budget. We experiment with the adaptive budget and show results in Table 4. We observe that this is a

| Model | Top-1 | Top-5 |
|----------------------|-------|-------|
| Simple MLP selector | 65.03 | 88.52 |
| Edges | 64.98 | 88.92 |
| Isolated peaks | 64.83 | 88.67 |
| Sharpen distribution | 64.80 | 87.98 |
| Global branch | 65.10 | 88.55 |

Table 5. **Results of impact of different variants** of data cleaning strategies and integration of global branch. Results are tested with 4K samples of the SS-V2 test set.

| Model | P-Ratio | GFLOPs | Top-1 | Top-5 |
|------------------|---------|--------|-------|-------|
| TimeSformer-B | 1 | 180 | 56.23 | 83.63 |
| TimeSformer-LITE | 0.9 | 158 | 56.00 | 83.37 |
| TimeSformer-LITE | 0.7 | 117 | 53.38 | 81.62 |
| TimeSformer-LITE | 0.5 | 79 | 48.28 | 77.62 |
| TimeSformer-LITE | 0.3 | 45 | 36.97 | 66.52 |
| TimeSformer-LITE | 0.1 | 15 | 11.68 | 29.54 |

Table 6. **Results of LITE on a different backbone on SS-V2 dataset.** While LITE is still able to retain accuracy in different backbones, the quality of the oracle is significantly worse, affecting the overall performance.

promising direction as the computation can be reduced by up to a third, while sacrificing $< 1\%$ in accuracy. We term this model LITE++, enabling further computational savings (additional results in Supplemental Material).

Variants. It is remarkable to see in Table 5 that none of the reasonable ideas from Sec. 4.4 significantly outperform a simple MLP. This points to a striking conclusion: the oracle is extremely hard to predict, and the MLP achieves a balance between accuracy and avoiding overfitting.

Experiments across backbones. We explore the effect of using a different backbone, the TimeSformer [2] and show results in Table 6. While for high P-Ratio values LITE can still preserve accuracy while reducing a large percentage of GFLOPs, the effect is less striking than using VideoMAE. This points to the fact that a less accurate backbone leads to a noisier oracle, affecting the overall performance of LITE.

6. Conclusion

We took a close look at the nature of video tokens to distill five interesting insights about what makes a token valuable for video understanding, how this value is distributed and how the number of tokens needed correlates to the difficulty of the task. We leverage these principles to design a token selector, which we call LITE, that outperforms the existing state-of-the-art in the trade-off between accuracy and computation. We hope both the principles as well as LITE can cast a new light into research on efficient Transformer-based video analysis models.

References

- [1] Anurag Arnab, Mostafa Dehghani, Georg Heigold, Chen Sun, Mario Lucic, and Cordelia Schmid. Vivit: A video vision transformer. *2021 IEEE/CVF International Conference on Computer Vision (ICCV)*, pages 6816–6826, 2021. 1, 3, 7
- [2] Gedas Bertasius, Heng Wang, and Lorenzo Torresani. Is space-time attention all you need for video understanding? *ArXiv*, abs/2102.05095, 2021. 7, 8
- [3] Gedas Bertasius, Heng Wang, and Lorenzo Torresani. Is space-time attention all you need for video understanding? In *ICML*, page 4, 2021. 3
- [4] Daniel Bolya, Cheng-Yang Fu, Xiaoliang Dai, Peizhao Zhang, Christoph Feichtenhofer, and Judy Hoffman. Token merging: Your ViT but faster. In *International Conference on Learning Representations*, 2023. 2, 3, 4, 7
- [5] Shyamal Buch, Cristóbal Eyzaguirre, Adrien Gaidon, Jiajun Wu, Li Fei-Fei, and Juan Carlos Niebles. Revisiting the “video” in video-language understanding. In *CVPR*, 2022. 3
- [6] Adrian Bulat, Juan-Manuel Pérez-Rúa, Swathikiran Sudhakaran, Brais Martínez, and Georgios Tzimiropoulos. Space-time mixing attention for video transformer. In *Neural Information Processing Systems*, 2021. 3
- [7] Joao Carreira and Andrew Zisserman. Quo vadis, action recognition? a new model and the kinetics dataset. In *proceedings of the IEEE Conference on Computer Vision and Pattern Recognition*, pages 6299–6308, 2017. 3
- [8] Joonmyung Choi, Sanghyeok Lee, Jaewon Chu, Minhyuk Choi, and Hyunwoo J. Kim. vid-tldr: Training free token merging for light-weight video transformer. In *Conference on Computer Vision and Pattern Recognition*, 2024. 2, 3
- [9] Shuangrui Ding, Peisen Zhao, Xiaopeng Zhang, Rui Qian, Hongkai Xiong, and Qi Tian. Prune spatio-temporal tokens by semantic-aware temporal accumulation. *2023 IEEE/CVF International Conference on Computer Vision (ICCV)*, pages 16899–16910, 2023. 2, 3, 4, 7
- [10] Alexey Dosovitskiy, Lucas Beyer, Alexander Kolesnikov, Dirk Weissenborn, Xiaohua Zhai, Thomas Unterthiner, Mostafa Dehghani, Matthias Minderer, Georg Heigold, Sylvain Gelly, et al. An image is worth 16x16 words: Transformers for image recognition at scale. In *International Conference on Learning Representations*, 2020. 3, 5
- [11] Haoqi Fan, Bo Xiong, Karttikeya Mangalam, Yanghao Li, Zhicheng Yan, Jitendra Malik, and Christoph Feichtenhofer. Multiscale vision transformers. *2021 IEEE/CVF International Conference on Computer Vision (ICCV)*, pages 6804–6815, 2021. 3
- [12] Christoph Feichtenhofer. X3d: Expanding architectures for efficient video recognition. *2020 IEEE/CVF Conference on Computer Vision and Pattern Recognition (CVPR)*, pages 200–210, 2020. 3
- [13] Christoph Feichtenhofer, Haoqi Fan, Jitendra Malik, and Kaiming He. Slowfast networks for video recognition. *2019 IEEE/CVF International Conference on Computer Vision (ICCV)*, pages 6201–6210, 2018. 3
- [14] Zhanzhou Feng, Jiaming Xu, Lei Ma, and Shiliang Zhang. Efficient video transformers via spatial-temporal token merging for action recognition. *ACM Transactions on Multimedia Computing, Communications and Applications*, 20: 1–21, 2023. 2, 3, 7
- [15] Shreyank N Gowda, Marcus Rohrbach, and Laura Sevilla-Lara. Smart frame selection for action recognition. In *Proceedings of the AAAI Conference on Artificial Intelligence*, pages 1451–1459, 2021. 3
- [16] Shreyank N Gowda, Xinyue Hao, Gen Li, Shashank Narayana Gowda, Xiaobo Jin, and Laura Sevilla-Lara. Watt for what: Rethinking deep learning’s energy-performance relationship. *arXiv preprint arXiv:2310.06522*, 2023. 1
- [17] Shreyank N Gowda, Anurag Arnab, and Jonathan Huang. Optimizing factorized encoder models: Time and memory reduction for scalable and efficient action recognition. In *European Conference on Computer Vision*, pages 457–474. Springer, 2025. 3
- [18] Raghav Goyal, Samira Ebrahimi Kahou, Vincent Michalski, Joanna Materzynska, Susanne Westphal, Heuna Kim, Valentin Haenel, Ingo Fründ, Peter N. Yianilos, Moritz Mueller-Freitag, Florian Hoppe, Christian Thureau, Ingo Bax, and Roland Memisevic. The “something something” video database for learning and evaluating visual common sense. *2017 IEEE International Conference on Computer Vision (ICCV)*, pages 5843–5851, 2017. 3
- [19] D. I. Kondratyuk, Liangzhe Yuan, Yandong Li, Li Zhang, Mingxing Tan, Matthew A. Brown, and Boqing Gong. Movinets: Mobile video networks for efficient video recognition. *2021 IEEE/CVF Conference on Computer Vision and Pattern Recognition (CVPR)*, pages 16015–16025, 2021. 3, 6
- [20] Rajat Koner, Gagan Jain, Prateek Jain, Volker Tresp, and Sujoy Paul. Lookupvit: Compressing visual information to a limited number of tokens. *ArXiv*, abs/2407.12753, 2024. 3, 7
- [21] Ze Liu, Yutong Lin, Yue Cao, Han Hu, Yixuan Wei, Zheng Zhang, Stephen Lin, and Baining Guo. Swin transformer: Hierarchical vision transformer using shifted windows. In *Proceedings of the IEEE/CVF international conference on computer vision*, pages 10012–10022, 2021. 3
- [22] Ze Liu, Jia Ning, Yue Cao, Yixuan Wei, Zheng Zhang, Stephen Lin, and Han Hu. Video swin transformer. *2022 IEEE/CVF Conference on Computer Vision and Pattern Recognition (CVPR)*, pages 3192–3201, 2021. 7
- [23] Daniel Neimark, Omri Bar, Maya Zohar, and Dotan Asselmann. Video transformer network. *2021 IEEE/CVF International Conference on Computer Vision Workshops (ICCVW)*, pages 3156–3165, 2021. 3
- [24] Bolin Ni, Houwen Peng, Minghao Chen, Songyang Zhang, Gaofeng Meng, Jianlong Fu, Shiming Xiang, and Haibin Ling. Expanding language-image pretrained models for general video recognition. In *European Conference on Computer Vision*, pages 1–18. Springer, 2022. 3
- [25] Junting Pan, Ziyi Lin, Xiatian Zhu, Jing Shao, and Hongsheng Li. St-adapter: Parameter-efficient image-to-video transfer learning. *Advances in Neural Information Processing Systems*, 35:26462–26477, 2022. 3

- [26] Seong Hyeon Park, Jihoon Tack, Byeongho Heo, Jung-Woo Ha, and Jinwoo Shin. K-centered patch sampling for efficient video recognition. In *European Conference on Computer Vision*, 2022. 3
- [27] Mandela Patrick, Dylan Campbell, Yuki M. Asano, Ishan Misra Florian Metze, Christoph Feichtenhofer, Andrea Vedaldi, and João F. Henriques. Keeping your eye on the ball: Trajectory attention in video transformers. In *Neural Information Processing Systems*, 2021. 2, 3, 7
- [28] David Patterson, Joseph Gonzalez, Urs Hölzle, Quoc Le, Chen Liang, Lluís-Miquel Munguia, Daniel Rothchild, David R. So, Maud Texier, and Jeff Dean. The carbon footprint of machine learning training will plateau, then shrink. *Computer*, 55(7):18–28, 2022. 1
- [29] Benjamin Peters, James J. DiCarlo, Todd M. Gureckis, Ralf Haefner, Leyla Isik, Joshua B. Tenenbaum, Talia Konkle, Thomas Naselaris, Kimberly L. Stachenfeld, Zenna Tavares, Doris Tsao, Ilker Yildirim, and Nikolaus Kriegeskorte. How does the primate brain combine generative and discriminative computations in vision? *CoRR*, abs/2401.06005, 2024. 6
- [30] Yongming Rao, Wenliang Zhao, Benlin Liu, Jiwen Lu, Jie Zhou, and Cho-Jui Hsieh. Dynamicvit: Efficient vision transformers with dynamic token sparsification. *Advances in neural information processing systems*, 34:13937–13949, 2021. 3
- [31] Michael S Ryoo, AJ Piergiovanni, Anurag Arnab, Mostafa Dehghani, and Anelia Angelova. Tokenlearner: What can 8 learned tokens do for images and videos? *arXiv preprint arXiv:2106.11297*, 2021. 3
- [32] Ramprasaath R. Selvaraju, Abhishek Das, Ramakrishna Vedantam, Michael Cogswell, Devi Parikh, and Dhruv Batra. Grad-cam: Visual explanations from deep networks via gradient-based localization. *International Journal of Computer Vision*, 128:336–359, 2016. 2, 4
- [33] Laura Sevilla-Lara, Shengxin Zha, Zhicheng Yan, Vedanuj Goswami, Matt Feiszli, and Lorenzo Torresani. Only time can tell: Discovering temporal data for temporal modeling. *2021 IEEE Winter Conference on Applications of Computer Vision (WACV)*, pages 535–544, 2019. 3
- [34] Zhan Tong, Yibing Song, Jue Wang, and Limin Wang. Videomae: Masked autoencoders are data-efficient learners for self-supervised video pre-training. *ArXiv*, abs/2203.12602, 2022. 3, 7
- [35] Hugo Touvron, Matthieu Cord, Matthijs Douze, Francisco Massa, Alexandre Sablayrolles, and Hervé Jégou. Training data-efficient image transformers & distillation through attention. In *International conference on machine learning*, pages 10347–10357. PMLR, 2021. 3
- [36] Ashish Vaswani, Noam Shazeer, Niki Parmar, Jakob Uszkoreit, Llion Jones, Aidan N Gomez, Łukasz Kaiser, and Illia Polosukhin. Attention is all you need. *Advances in neural information processing systems*, 30, 2017. 1, 3
- [37] Junke Wang, Xitong Yang, Hengduo Li, Zuxuan Wu, and Yu-Gang Jiang. Efficient video transformers with spatial-temporal token selection. In *European Conference on Computer Vision*, 2021. 3, 7
- [38] Mengmeng Wang, Jiazheng Xing, Jianbiao Mei, Yong Liu, and Yunliang Jiang. Actionclip: Adapting language-image pretrained models for video action recognition. *IEEE Transactions on Neural Networks and Learning Systems*, 2023. 3
- [39] Xijun Wang, Junbang Liang, Chun-Kai Wang, Kenan Deng, Yu (Michael) Lou, Ming Lin, and Shan Yang. Vila: Efficient video-language alignment for video question answering. In *ECCV*, 2024. 3
- [40] Syed Talal Wasim, Muhammad Uzair Khattak, Muzammal Naseer, Salman Khan, Mubarak Shah, and Fahad Shahbaz Khan. Video-focalnets: Spatio-temporal focal modulation for video action recognition. In *Proceedings of the IEEE/CVF International Conference on Computer Vision*, pages 13778–13789, 2023. 3
- [41] Chao-Yuan Wu, Manzil Zaheer, Hexiang Hu, R. Manmatha, Alex Smola, and Philipp Krähenbühl. Compressed video action recognition. *2018 IEEE/CVF Conference on Computer Vision and Pattern Recognition*, pages 6026–6035, 2017. 3
- [42] Chao-Yuan Wu, Yanghao Li, Karttikeya Mangalam, Haoqi Fan, Bo Xiong, Jitendra Malik, and Christoph Feichtenhofer. Memvit: Memory-augmented multiscale vision transformer for efficient long-term video recognition. *2022 IEEE/CVF Conference on Computer Vision and Pattern Recognition (CVPR)*, pages 13577–13587, 2022. 3
- [43] Taojiannan Yang, Yi Zhu, Yusheng Xie, Aston Zhang, Chen Chen, and Mu Li. Aim: Adapting image models for efficient video action recognition. In *The Eleventh International Conference on Learning Representations*, 2023. 3
- [44] Hongxu Yin, Arash Vahdat, José Manuel Álvarez, Arun Mallya, Jan Kautz, and Pavlo Molchanov. A-vit: Adaptive tokens for efficient vision transformer. *2022 IEEE/CVF Conference on Computer Vision and Pattern Recognition (CVPR)*, pages 10799–10808, 2021. 3
- [45] Shoubin Yu, Jaemin Cho, Prateek Yadav, and Mohit Bansal. Self-chained image-language model for video localization and question answering. In *NeurIPS*, 2024. 3
- [46] Ting Zhao and Xiangqian Wu. Pyramid feature attention network for saliency detection. In *IEEE Conference on Computer Vision and Pattern Recognition (CVPR)*, 2019. 4
- [47] Xingyi Zhou, Anurag Arnab, Chen Sun, and Cordelia Schmid. How can objects help action recognition? *2023 IEEE/CVF Conference on Computer Vision and Pattern Recognition (CVPR)*, pages 2353–2362, 2023. 7
- [48] Mohammadreza Zolfaghari, Kamaljeet Singh, and Thomas Brox. Eco: Efficient convolutional network for online video understanding. *ArXiv*, abs/1804.09066, 2018. 3